life

MDPI

*Article*

# Multimodal Structural Micro-Analysis of DOT® Polynucleotide (PN) and DOT® Polydeoxyribonucleotide (PDRN): An Exploratory Qualitative Study

**Michael James Kim [1], Yu-Na Kim [2], Kyoung-Hee Kim [2], Kyungeun Lee [3], Chee-Youb Won [1], Subin Weon [1], Jin Hyun Kim [4] and Kyu-Ho Yi [4,*]**

[1] Integrated R&D Center, Pharmaresearch Co., Ltd. 22, Geumto-Ro 40beon-Gil, Sujeoung-Gu, Sungnam 13453, Republic of Korea
[2] SCAI Therapeutics Co., Ltd., A105, 17, Techno 4-Ro, Yuseong-Gu, Daejeon 34013, Republic of Korea
[3] Advanced Analysis and Data Center, Korea Institute of Science and Technology, 5, Hwarang-Ro 14-Gil, Seongbuk-Gu, Seoul 02792, Republic of Korea
[4] Division in Anatomy and Developmental Biology, Department of Oral Biology, Human Identification Research Institute, BK21 FOUR Project, Yonsei University College of Dentistry, Seoul 03722, Republic of Korea
* Correspondence: kyuho90@daum.net; Tel.: +82-2-2228-3047; Fax: +82-2-393-8076

**Abstract**

Background: The microscopic appearances of polynucleotide (PN) and polydeoxyribonucleotide (PDRN) formulations have been interpreted as evidence of different supramolecular architectures, but formulation and preparation effects remain unresolved. Objective: To describe the available multimodal observations of DOT® PN and DOT® PDRN without assuming that they establish an intrinsic or functional scaffold. Methods: The formulations were examined by SYBR Green I confocal microscopy after purification, freeze-drying and reconstitution; high-pressure freezing cryogenic scanning electron microscopy (HPF cryo-SEM); and cryogenic transmission electron microscopy (cryo-TEM) after liquid ethane vitrification. Dried-film X-ray diffraction (XRD) was also performed, but its incompletely labeled graphical record was not retained as confirmatory evidence. Comparisons were qualitative. Results: The selected confocal and HPF cryo-SEM images showed more reticulated appearances for PN than for PDRN. Cryo-TEM images showed overlapping strand-like features in PN and more dispersed features in PDRN. These observations were not supported by quantitative morphometry, documented independent replication or a fully presented concentration-matched comparison. A reported diluted-PN observation lacked a corresponding image dataset and was not used to exclude concentration effects. Conclusions: The images describe preparation-specific morphological appearances of the examined formulations. They do not establish PN-specific native architecture, hydrated-state anisotropy, comparative stability or scaffold function. The findings are exploratory and cannot be generalized to PN and PDRN as material classes or used to infer clinical performance.

**Keywords:** polynucleotide; polydeoxyribonucleotide; qualitative microscopy; confocal microscopy; high-pressure freezing; cryo-SEM; cryo-TEM; sample preparation; morphological characterization

Check for updates

Academic Editor: Fei Fan

Received: 26 September 2026
Revised: 5 November 2026
Accepted: 10 November 2026
Published: 26 November 2026

**Copyright:** © 2026 by the authors. Licensee MDPI, Basel, Switzerland. This article is an open access article distributed under the terms and conditions of the Creative Commons Attribution (CC BY) license.

## 1. Introduction

Polynucleotide (PN) and polydeoxyribonucleotide (PDRN) formulations are discussed as nucleic-acid-based injectable materials with differing molecular and clinical characteristics [1–3]. Clinical reports have examined PN in skin rejuvenation, post-thyroidectomy scars,

periocular treatment and facial erythema [4–7]. Pharmacological activity has also been reviewed for PDRN [8]. These reports provide context for studying formulation morphology, but they do not establish that a particular microscopic pattern causes a clinical effect or that the samples examined here have the characteristics reported for other preparations.

Kim et al. described high-resolution three-dimensional scanning electron microscopy (SEM) images of DOT® (DNA Optimizing Technology) PN and DOT® PDRN [1]. Their PN images were interpreted as a polygonal, scaffold-like pattern, whereas PDRN appeared comparatively amorphous. That report motivates a closer examination of whether similar appearances occur with other preparation and imaging methods. It does not provide an independent measurement of the molecular-weight distribution or fragment lengths of the samples in the present study.

Preparation is particularly important when interpreting water-rich materials. Freezing, etching and related processing may influence the morphology visible in electron microscopy; high-pressure freezing is intended to reduce ice-crystal formation, not to eliminate every source of structural alteration [9–11]. Cryo-TEM after vitrification provides another observational approach [12]. Polymer organization also depends on the conditions under which chains are examined [13]. Consequently, agreement between selected images obtained by different methods is informative but cannot substitute for concentration-matched controls, material characterization or independent replication.

The objective of this exploratory in vitro study was to describe the appearances of the examined DOT® PN and DOT® PDRN samples using confocal microscopy, HPF cryo-SEM and cryo-TEM. The record also included dried-film XRD, whose interpretive limitations are reported separately. The study does not test whether PN possesses a unique native scaffold, whether a network has a material or biological function, or whether the formulations differ in clinical efficacy. The terms "reticulated," "strand-like" and "network-like" are used as descriptions of image appearance, not as proof of molecular topology, crosslinking or scaffold function.

## 2. Materials and Methods

### *2.1. Study Scope and Material Characterization*

DOT® PN and DOT® PDRN were examined as formulations in a qualitative in vitro materials-characterization study. The cryo-TEM comparison was described using nominal PN at 2% *w*/*v* and PDRN at approximately 0.2% *w*/*v*. These concentrations were not matched. The confocal preparation followed a separate dilution and reconstitution workflow, described below; the cryo-TEM concentrations must not be assumed to apply to the confocal images.

The available material description does not specify nucleotide sequences, fragment-length or base-pair distributions, measured molecular-weight distributions, product-lot identifiers, ionic composition or excipient concentrations. The labels PN and PDRN therefore identify the formulations under study rather than analytically matched, sequence-defined oligonucleotides. No matched vehicle-control dataset, molecular-weight-matched generic DNA comparator or independently replicated product-lot comparison is documented in this report. No sequence, chain length or molecular weight has been assigned from the images or imported from another study as a measurement of these samples.

### *2.2. Sybr Green I Confocal Microscopy*

For confocal imaging, PN or PDRN was prepared at 100 mg in 10 mL distilled water, corresponding to a nominal initial concentration of 1% *w*/*v* before staining and subsequent processing. SYBR Green I (10 µg) was added as a fluorescent marker. After binding, unbound dye was removed by purification, the material was freeze-dried, and the dye-

bound sample was re-dissolved for imaging. Images were acquired on a STELLARIS 8 super-resolution confocal system using Lightning mode. Low- and high-magnification fields were examined to describe spatial distribution and reticulated fluorescence.

The available methods record does not specify the purification procedure, reconstitution volume or final concentration, equilibration time, or the pH and buffer composition after reconstitution. No direct staining comparison on the hydrated formulation without intermediate freeze-drying is documented, and the record does not establish why that alternative was not used. Accordingly, the confocal images are observations of processed, reconstituted samples, not direct measurements of unprocessed commercial gels. Final imaging concentrations cannot be inferred from the initial mass and volume alone. The labeling procedure was used for visualization and was not a reported assay of nucleic-acid purity or integrity.

### *2.3. High-Pressure Freezing Cryo-Sem*

In the HPF workflow, gel samples were loaded into 6-mm aluminum carriers and frozen under approximately 2100 bar using an HPM100 system before transfer for etching and coating. After preparation, specimens were examined on a Quanta 3D FEG Cryo-FIB/SEM platform. Surface and section images were obtained after controlled etching and Pt/Pd coating.

HPF was used to reduce crystalline-ice formation during preparation [9–11]. The images were interpreted as appearances after freezing, etching and coating. Method-specific formulation concentrations, etching and coating settings, and the number of independent HPF preparations are not fully documented. The HPF workflow does not document an ethane-immersion step, but it is not a matched before-and-after ethane stability experiment.

### *2.4. Cryo-Tem and the Reported Dilution Condition*

One-microliter aliquots were vitrified in liquid ethane on Quantifoil grids using a Vitrobot Mark IV operated at 8 °C and 100% humidity, with a blot time of 3.5 s. Images were obtained on a 200-kV Glacios microscope from electron-transparent grid regions. Fast Fourier transform (FFT) insets were inspected qualitatively for features relevant to ice preparation [12]. Liquid ethane was used as a cryogen during specimen preparation, not as a omponent of a therapeutic delivery system.

A supplementary PN condition at approximately 0.2% *w/v* was described in the study record as approximating the nominal PDRN concentration. However, no separately identifiable image panel, complete image dataset or quantitative analysis for that condition accompanies the report. Its reported observation is therefore not used as evidence that concentration effects were controlled. Figure 3 does not present a three-condition comparison of PN 2%, PN 0.2% and PDRN 0.2%. No direct pre-/post-vitrification molecular-stability assay or matched non-ethane stability control is documented.

### *2.5. Dried-Film Xrd: Recorded Procedure and Interpretive Restriction*

For diffraction analysis, thin films were prepared by spreading the sample on a cover glass and drying for 24 h on a 55 °C hotplate under airflow-restricted conditions. Conventional XRD scans were recorded on a MiniFlex instrument over 3–60° 2θ at 5°/min with 0.02° step width.

Pole-figure analysis was performed on a SmartLab system at 2θ = 24.78° with Cu Kα radiation; the original acquisition description designated this as the 001 reflection. No additional crystallographic indexing validation is provided here. The available diffraction graphic has incomplete intensity-axis labels and partially obscured pole-figure scales. Raw numerical intensities, normalization procedures, replicate scans and quantitative orientation

analyses do not accompany this report. The graphic is therefore not reproduced as interpretable comparative evidence, and no missing values or units have been reconstructed. The acquisition procedure is retained for transparency, but diffraction does not support the conclusions of the revised report.

### *2.6. Image Interpretation, Replication and Statistical Scope*

All microscopy comparisons were qualitative assessments of the selected images. The available record does not provide the numbers of independent preparations, grids, fields or product lots, or a documented random or blinded field-selection procedure. These numbers and procedures have not been inferred. Multiple views, magnifications or imaging methods are not treated as independent biological or material replicates.

No distributions of pore or mesh area, calibrated fiber diameters, connectivity measurements or orientation order parameters are reported. Formal statistical comparisons, confidence intervals and between-lot uncertainty estimates are not available. Approximate dimensions already recorded for selected confocal fields are identified as visual estimates in the Results, not as quantitative validation of a material difference. Image morphology is not used to infer chemical stability, molecular fragment length, degradation resistance or mechanical performance.

## 3. Results

### *3.1. Confocal Appearances After Processing and Reconstitution*

In the selected confocal images, PN displayed a reticulated fluorescent appearance with bright strand-like features around darker intervals. PDRN showed more separated fluorescent domains with less apparent continuity (Figure 1). These descriptions apply to the displayed processed samples and do not establish differences in native gel architecture or viscosity. The overall brightness was not used as a quantitative comparison of polymer concentration or purity.

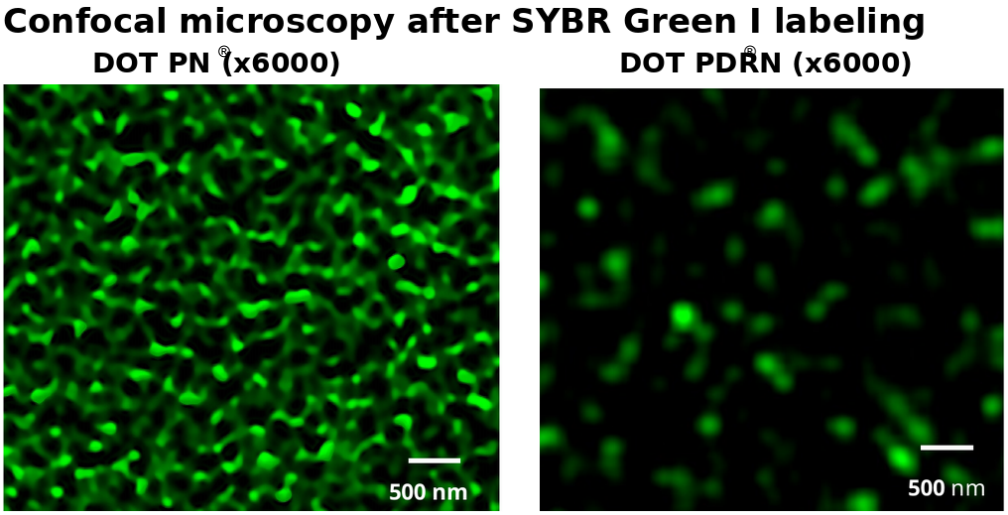


**Figure 1.** Confocal appearances of processed samples after SYBR Green I labeling, purification, freeze-drying and reconstitution. (**Left**) DOT® PN, with reticulated fluorescence. (**Right**) DOT® PDRN, with more separated fluorescent domains. The source panels are labeled 6000×; the displayed scale bars are 500 nm. Final post-reconstitution concentrations are not documented. These selected images illustrate morphology after the stated processing and do not establish native structure, molecular fiber diameter or a statistically supported difference.

Approximate visual estimates reported for selected confocal fields were 450–600 nm for pore-like intervals and 72–160 nm for fluorescent-feature widths. These estimates were not accompanied by a defined sampling count, a measurement distribution or uncertainty estimates. Fluorescent-feature width was recognized to depend on local intensity and optical rendering; it is not interpreted as a validated diameter of an individual DNA chain or polymer fiber. The estimates are retained as descriptive observations only.

### *3.2. Hpf Cryo-Sem Appearances*

The displayed HPF cryo-SEM fields at 50,000× and 100,000× showed a more closely arranged reticular appearance in PN than in PDRN, whose visible features appeared less compact (Figure 2). Apparent continuity and density were judged visually; they were not quantified as connectivity, fiber density or mesh-size distributions. These images do not show that every field or product lot behaves similarly, that preparation artifacts have been eliminated, or that a functional scaffold has been demonstrated.

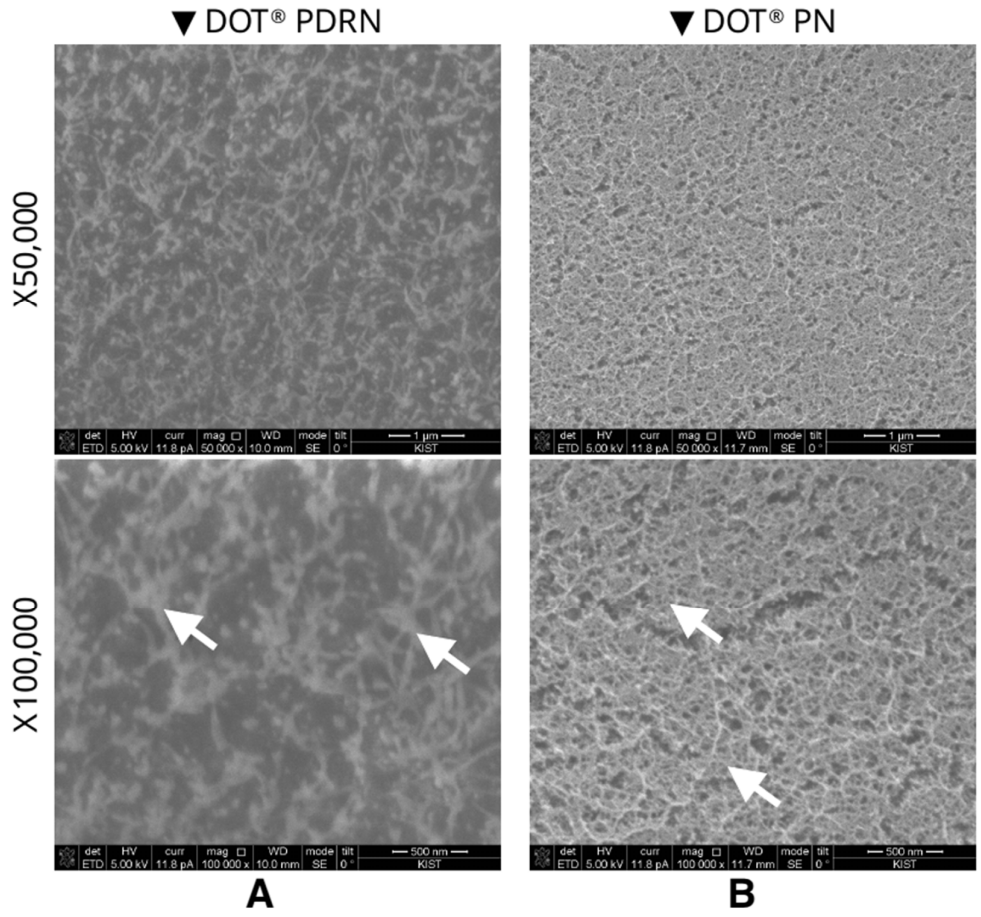


**Figure 2.** HPF cryo-SEM images after freezing, etching and Pt/Pd coating. Column (**A**) DOT® PDRN. Column (**B**) DOT® PN. The upper and lower rows are labeled 50,000× and 100,000×, respectively. Source scale bars are 1 µm in the upper row and 500 nm in the lower row. White arrows identify selected visible reticular features and are not quantitative measurements. The panels illustrate the appearances of the processed specimens; matched method-specific concentrations, independent sample counts and between-lot reproducibility are not established by this figure.

### *3.3. Cryo-Tem Appearances After Liquid Ethane Vitrification*

The selected PN cryo-TEM field contained elongated strand-like features with areas of apparent overlap, whereas the PDRN field showed more dispersed and less continuous features (Figure 3). These descriptions concern image projections, not measured nucleotide

lengths or demonstrated three-dimensional connectivity. The FFT insets showed concentric ring-like features without obvious sharp crystalline spots. This qualitative observation does not establish that all preparation effects were absent or that the polymers retained their original chemical or molecular integrity.

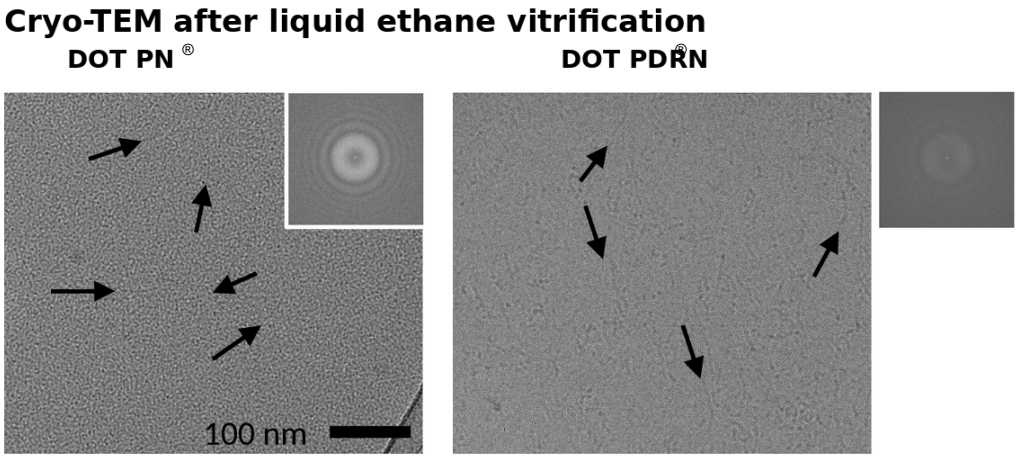


**Figure 3.** Cryo-TEM after liquid ethane vitrification. (**Left**) DOT® PN. (**Right**) DOT® PDRN. Black arrows indicate selected strand-like image features; insets show FFT patterns from the source presentation. The supplied 100-nm scale bar applies to the PN panel. A separately documented scale calibration for the displayed PDRN panel is not available, so the panels are not used for quantitative cross-material size comparison. No PN 0.2% panel is included. The images and FFT insets do not constitute a concentration-matched control or an assay of polymer integrity.

### *3.4. Observations Excluded from Confirmatory Interpretation*

The study record described persistent strand-like features in diluted PN, but this observation cannot be independently evaluated from the figures presented and does not resolve the concentration imbalance. The dried-film diffraction presentation also suggested visually different profiles and color distributions, but the incomplete axes and scales prevent a reliable numerical interpretation. No diffraction-derived intensity difference, orientation angle, crystallinity comparison or anisotropy parameter is reported. Neither observation is used to establish an intrinsic difference between PN and PDRN.

## 4. Discussion

### *4.1. What the Microscopy Observations Support*

The available microscopy panels show preparation-specific differences in the appearances of the examined formulations. PN appears more reticulated in the confocal and HPF cryo-SEM panels and displays overlapping strand-like features in the cryo-TEM panel. This is a limited descriptive observation, not a demonstration of a reproducible material-class distinction. Similar-looking features across methods may guide a hypothesis, but the absence of documented independent sampling prevents their frequency and robustness from being estimated.

The earlier SEM report proposed a scaffold-like interpretation of a polygonal PN appearance [1]. The present selected images permit discussion of a reticular or strand-like appearance under other preparation conditions. They do not validate the earlier scaffold claim, establish that its geometric pattern was an artifact, or resolve the native architecture of PN. No direct, controlled comparison of the earlier and current preparation workflows is reported. The earlier and present observations should therefore be interpreted within their respective sample-preparation conditions.

### *4.2. Formulation, Concentration and Hydration as Unresolved Variables*

The nominal 2% PN versus approximately 0.2% PDRN comparison includes a tenfold concentration difference. The unillustrated diluted-PN observation does not provide a documented concentration-matched control. In addition, the absence of sample-specific fragment-length distributions, molecular-weight measurements, ionic composition and excipient information prevents a separation of chain-related, concentration-related and formulation-related explanations. Literature descriptions of longer PN chains or shorter PDRN fragments [1,3,8] cannot substitute for measurements of the materials examined here.

Solvation, including hydration in aqueous preparations, is an important interpretive consideration rather than a measured property of these samples. Water–polymer interactions and solution conditions may contribute to the organization of polymer systems [13], but no hydration-shell structure, bound-water fraction or water-mobility measurement is reported for PN or PDRN. The samples also experienced different histories: confocal preparations were freeze-dried and reconstituted, electron-microscopy preparations were frozen, and the diffraction specimens were dried at 55 °C. These states cannot be treated as equivalent observations of the same native hydrated network. The present data do not establish that PN has a thicker hydration shell, greater water retention or greater hydration-mediated stability than PDRN.

Vehicle controls, generic DNA preparations matched for molecular weight, matched concentration series and independent product lots would be required to distinguish a formulation-specific appearance from more general polymer behavior. Those comparisons are not documented in the present report. Thus, the images cannot establish a DOT®-specific effect or support generalization to all PN and PDRN preparations.

### *4.3. Preparation Effects, Liquid Ethane and Material Stability*

Freezing and microscopy preparation can influence the observed appearance of soft materials [9–12]. HPF and liquid ethane vitrification are different preparation approaches, but observations after one approach are not a controlled stability comparison for the other. The absence of a documented ethane step in the HPF workflow does not show that ethane had no effect on the cryo-TEM specimens. FFT appearance is likewise not a molecular-integrity assay. A matched comparison with an alternative preparation or a pre-/post-processing integrity measurement is not reported.

The confocal workflow has a separate limitation: purification, freeze-drying and reconstitution intervene between the original preparation and imaging. Without documented reconstitution conditions and a direct-staining comparator, the extent to which the displayed fluorescence reflects the starting hydrated material cannot be determined. Preservation of conformation cannot be assumed. The absence of a documented rationale for omitting direct in situ staining is a further reporting limitation.

Chemical stability, resistance to enzymatic degradation, persistence of morphology over time and mechanical stability are different outcomes. None is established by a single selected image or by the apparent compactness of a reticular pattern. No time-course, storage-stability, enzymatic-challenge or pre-/post-vitrification degradation dataset is reported. Consequently, the observations cannot rank the stability of PN and PDRN or predict comparative tissue residence.

### *4.4. Rna-Related Uncertainty, Delivery and the Meaning of "Scaffold"*

The investigated formulations are discussed as DNA-based PN/PDRN materials, not as sequence-defined RNA therapeutics [3,8]. Nevertheless, no RNA-specific purity assessment or RNase/DNase challenge is documented for the examined samples. The fluorescent images therefore do not exclude RNA carryover, establish whether enzymatic degradation

occurred, or demonstrate resistance to nuclease activity. These questions remain unresolved rather than being dismissed on the basis of product terminology.

The study does not evaluate a nucleic-acid delivery system. No therapeutic carrier, cellular uptake experiment, intracellular delivery assay or release measurement is described; the confocal dye is an imaging label and liquid ethane is a preparation cryogen. Accordingly, the images support no conclusion about intracellular nucleic-acid activity, nutrient-mediated effects, receptor signaling or comparative therapeutic mechanisms. Clinical and pharmacological literature [3–8] is background context, not functional evidence for these particular samples.

In this report, "network-like" refers to visible morphology. A functional scaffold would require evidence beyond that appearance, such as a relevant physical or biological performance measurement. The present report contains no rheology, load-bearing, diffusion, cell-support or tissue-interaction data. It therefore neither demonstrates scaffold function nor replaces a polygonal scaffold model with a validated fibrous scaffold model.

### *4.5. Dried-Film Diffraction Does Not Establish Native Anisotropy*

The XRD specimens were thin films produced by heating and drying on glass. Organization after this treatment cannot be assumed to represent the hydrated injectable formulation. Drying-related alignment remains an alternative explanation that the present study does not separate from any pre-existing organization. The inadequately labeled graphical record, undocumented normalization and absence of replicate-level diffraction data further prevent a reproducible intensity or orientation comparison. For these reasons, the original diffraction figure has been withdrawn and claims of preferential native molecular orientation or intrinsic anisotropy have been removed.

Replicated, normalized diffraction and quantitative orientation analysis would be needed to support an interpretation of the dried films. Hydrated-state observations, such as appropriately designed small-angle scattering or polarized microscopy, together with relevant rheological measurements, would address a different question: whether any ordering or network organization persists in the formulation before drying and has a measurable physical consequence. No such validation is presented here.

### *4.6. Limits of Inference and Priorities for Further Work*

The principal limitations are not resolved by using several imaging modalities. Material matching and characterization are incomplete; the numbers and independence of sampled preparations, fields, grids and lots are not documented; image selection is not reported as randomized or blinded; and complete raw image datasets are not supplied. Quantitative morphometry and its uncertainty cannot be reconstructed reliably from the selected manuscript panels. These limitations constrain the main comparison itself, not only its precision.

A future confirmatory study would need characterized materials and appropriate controls at matched concentrations; independent product lots and sample preparations; prespecified, blinded image sampling; calibrated morphometry with uncertainty and statistical analysis at the appropriate independent-sample level; and accessible raw datasets. Hydrated-state physical measurements and defined stability assays would be necessary before attributing functional significance to an image pattern. These are requirements for testing the hypotheses raised here, not experiments or results supplied by the present revision. Commercial affiliations and the recorded participation of company-affiliated authors are disclosed below; independent validation would be particularly useful for a comparison of branded formulations.

## 5. Conclusions

Selected confocal, HPF cryo-SEM and cryo-TEM images show different qualitative appearances of the examined DOT® PN and DOT® PDRN formulations under the reported preparation conditions. The observations do not establish that the differences are independent of concentration, formulation composition or processing. They also do not demonstrate native hydrated-state anisotropy, molecular or enzymatic stability, or functional scaffold properties. The study is exploratory and hypothesis-generating; a reproducible intrinsic PN–PDRN architectural distinction remains to be tested using matched, characterized materials and independent quantitative measurements.

**Author Contributions:** Conceptualization: M.J.K., C.-Y.W. and K.-H.Y. Writing—Original Draft Preparation: S.W. and K.-H.Y. Writing—Review and Editing: M.J.K., Y.-N.K., K.-H.K., K.L., C.-Y.W., S.W., K.-H.Y. and J.H.K. Visualization: K.L. and S.W. Supervision: M.J.K., C.-Y.W., K.-H.Y. and J.H.K. All authors have read and agreed to the published version of the manuscript.

**Funding:** This study was funded by PharmaResearch Co., Ltd.

**Institutional Review Board Statement:** Not applicable. Ethical approval was not required because this was an in vitro materials-characterization study that did not involve human participants, human tissue, animals, clinical interventions or identifiable personal data.

**Informed Consent Statement:** Not applicable. This study did not involve human participants or clinical images.

**Data Availability Statement:** The data used in this study were provided by PharmaResearch Co., Ltd. The present report contains selected image panels and the methodological information described above. Complete raw imaging datasets, raw diffraction intensities and associated sample-level acquisition and replication metadata are not supplied with this report. Consequently, the complete underlying observations and their reproducibility cannot be independently assessed from the material presented.

**Conflicts of Interest:** Michael James Kim, Chee-Youb Won and Subin Weon list affiliations with Pharmaresearch Co., Ltd.; Yu-Na Kim and Kyoung-Hee Kim list affiliations with SCAI Therapeutics Co., Ltd. These are potentially relevant commercial relationships in a comparison of branded formulations. As specified in Author Contributions, company-affiliated authors participated in conceptualization, original drafting, review and editing, visualization and supervision. The contribution statement does not separately identify experimental execution or data-analysis responsibilities, and any additional organizational role in material or equipment provision, oversight or the decision to publish is not separately documented. This study received funding from PharmaResearch Co., Ltd., which also provided the data used in this study.

## References

1. Kim, M.J.; Park, H.-J.; Jung, R.-J.; Won, C.-Y.; Ohk, S.-O.; Kim, H.-T.; Roh, N.-K.; Yi, K.-H. High-resolution 3-D scanning electron microscopy (SEM) images of DOT® polynucleotides (PN): Unique scaffold characteristics and potential applications in biomedicine. *Ski. Res. Technol.* **2024**, *30*, e13667. [CrossRef]
2. Yi, K.-H.; Kang, H.; Song, J.K.; Sydorchuk, O.; Green, J.B.; Cartier, H.; Zamin, R.Z.; Ascher, B. Skin boosters: 2026 updated. *J. Cosmet. Dermatol.* **2026**, *25*, e70875. [CrossRef]
3. Kim, S.T. Comparison of polynucleotide and polydeoxyribonucleotide in dermatology: Molecular mechanisms and clinical perspectives. *Pharmaceutics* **2025**, *17*, 1024. [CrossRef]
4. Park, K.Y.; Seok, J.; Rho, N.K.; Kim, B.J.; Kim, M.N. Long-chain polynucleotide filler for skin rejuvenation: Efficacy and complications in five patients. *Dermatol. Ther.* **2016**, *29*, 37–40. [CrossRef]
5. Kim, J.H.; Jeong, J.J.; Lee, Y.I.; Lee, W.J.; Lee, C.; Chung, W.Y.; Nam, K.; Lee, J.H. Preventive effect of polynucleotide on post-thyroidectomy scars: A randomized, double-blinded, controlled trial. *Lasers Surg. Med.* **2018**, *50*, 755–762. [CrossRef]
6. Lee, Y.J.; Kim, H.T.; Lee, Y.J.; Paik, S.H.; Moon, Y.S.; Lee, W.J.; Chang, S.E.; Lee, M.W.; Choi, J.H.; Jung, J.M.; et al. Comparison of the effects of polynucleotide and hyaluronic acid fillers on periocular rejuvenation: A randomized, double-blind, split-face trial. *J. Dermatol. Treat.* **2022**, *33*, 254–260. [CrossRef]

7. Lee, D.; Kim, M.J.; Park, H.J.; Rah, G.C.; Choi, H.; Anh, S.; Ji, G.H.; Kim, M.S.; Kim, G.; Shin, D.W.; et al. Current practices and perceived effectiveness of polynucleotides for treatment of facial erythema by cosmetic physicians. *Ski. Res. Technol.* **2023**, *29*, e13466. [CrossRef]
8. Squadrito, F.; Bitto, A.; Irrera, N.; Pizzino, G.; Pallio, G.; Minutoli, L.; Altavilla, D. Pharmacological activity and clinical use of PDRN. *Front. Pharmacol.* **2017**, *8*, 224. Correction in *Front. Pharmacol.* **2022**, *13*, 1073510. https://doi.org/10.3389/fphar.2022.1073510. [CrossRef]
9. Echlin, P. *Low-Temperature Microscopy and Analysis*; Plenum Press: London, UK, 1992; pp. 35–92.
10. Sartori, N.; Richter, K.; Dubochet, J. Vitrification depth can be increased more than 10-fold by high pressure freezing. *J. Microsc.* **1993**, *172*, 55–61. [CrossRef]
11. Severs, N.J.; Terence, M.N.; Shotton, D.M. A practical introduction to rapid freezing techniques. In *Rapid Freezing, Freeze Fracture and Deep Etching*; Severs, N.J., Shotton, D.M., Eds.; Wiley-Liss: New York, NY, USA, 1995; pp. 31–49.
12. Dubochet, J.; Adrian, M.; Chang, J.-J.; Homo, J.-C.; Lepault, J.; McDowall, A.W.; Schultz, P. Cryo-electron microscopy of vitrified specimens. *Q. Rev. Biophys.* **1988**, *21*, 129–228. [CrossRef]
13. Rubinstein, M.; Colby, R.H. *Polymer Physics*; Oxford University Press: Oxford, UK, 2003.

**Disclaimer/Publisher's Note:** The statements, opinions and data contained in all publications are solely those of the individual author(s) and contributor(s) and not of MDPI and/or the editor(s). MDPI and/or the editor(s) disclaim responsibility for any injury to people or property resulting from any ideas, methods, instructions or products referred to in the content.